Electronic Supplementary Material (ESI) for Chemical Science.

Supporting Information for "Machine Learning Demonstrates the Impact of Proton Transfer and Solvent Dynamics on CO_2 Capture in Liquid Ammonia"

Marcos Calegari Andrade,* Sichi Li,* Tuan Anh Pham, Sneha A. Akhade, and Simon H. Pang*

Materials Science Division, Lawrence Livermore National Laboratory, Livermore, California 94550, United States

E-mail: calegariandr1@llnl.gov; li77@llnl.gov; pang6@llnl.gov

Further validation of the deep neural network potential

This section provides further support on the accuracy of the deep neural network potential (DP) developed in this work. Both the free energy surface and its first derivative with respect to the collective variable (reaction progress) derived from DP are directly compared with results obtained with the density functional SCAN. The excellent agreement between both methods is shown in Fig. S1, suggesting that the DP can accurately describe energies and forces of the system across the whole sampled potential energy surface, including those that involve charge separation and short-range electrostatics. The collective variable S shown in Fig. S1 is identical to the "reaction progress" described in the main text.

Since the calculation of the free energy surface (FES) of the CO_2 chemisoprtion in liquid

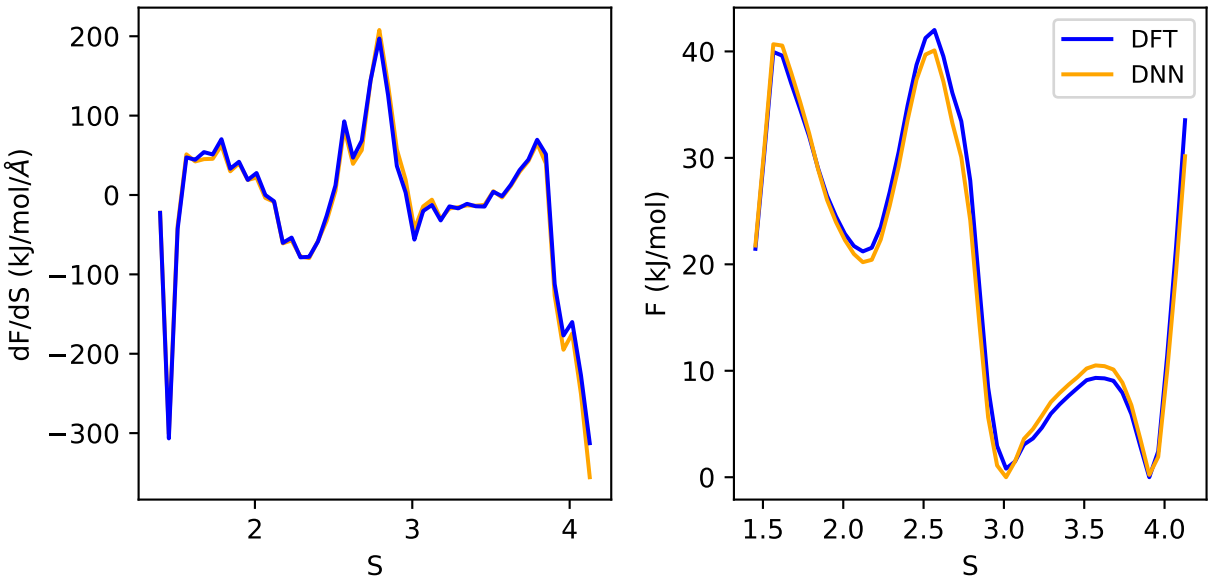

Figure S1: Comparison between the average generalized CV force (left) and the free energy surface (right) between DFT and the deep neural network potential (DP). The symbol "F" represents the free energy, while the "S" is the same collective variable labeled "reaction progress" in the main text.

ammonia requires extensive sampling using metadynamics. Such extensive sampling is not feasible with density functional theory (DFT). The calculation of the DFT FES was instead obtained from thermodynamics integration of the average generalized collective variable (CV) force:

$$F(S) = -\int_{S_0}^{S} \left\langle \frac{\partial U(\boldsymbol{r}^N)}{\partial S'} \right\rangle dS' \tag{S1}$$

with $U(\boldsymbol{r}^N)$ the potential energy surface, S the CV, S_0 the initial CV value and $\langle ... \rangle$ an ensemble average.

A set of 1000 configurations equally spaced in CV space were extracted from enhanced sampling using DP. Atomic forces were computed for each configuration and used to derive analytically the generalized collective variable (CV) force. This derivation is explicitly shown in the section below.

Derivation of the generalized force

For completeness, this section provides the derivation of the analytical expression of the generalized CV forces using Lagrange multipliers.[1,2]

We use an extended Lagrangean L with a multiplier λ, a set of 3N atomic coordinates $\boldsymbol{X}$, a set of atomic momenta $\boldsymbol{P}$, a collective variable $S(\boldsymbol{X})$, its target value S, kinetic energy K and the potential energy U.

$$L(\boldsymbol{X}, \boldsymbol{P}, \lambda) = K(P) - U(X) - \lambda\Big(S(X) - S\Big) \tag{S2}$$

The equations of motion derived from this Lagrangean are:

$$\dot{\boldsymbol{x}}_i = \boldsymbol{p}_i / m_i \tag{S3}$$

$$\dot{\boldsymbol{p}}_i = \boldsymbol{F}_i - \lambda \frac{\partial S(X)}{\partial \boldsymbol{x}_i} \tag{S4}$$

$$\dot{\lambda} = \sum_i \dot{\boldsymbol{x}}_i \frac{\partial S(X)}{\partial \boldsymbol{x}_i} \tag{S5}$$

$$\ddot{\lambda} = \sum_i \frac{\dot{\boldsymbol{p}}_i}{m_i} \frac{\partial S(X)}{\partial \boldsymbol{x}_i} + \sum_{ij} \frac{\boldsymbol{p}_i}{m_i} \frac{\partial^2 S(X)}{\partial \boldsymbol{x}_i \partial \boldsymbol{x}_j} \tag{S6}$$

Solving for the constraint $S(X) - S = 0$ with $\dot{\lambda} = 0$, $\ddot{\lambda} = 0$, and using S8 into S10,

$$\ddot{\lambda} = \sum_i \frac{1}{m_i} \left(\boldsymbol{F}_i - \frac{\partial S(X)}{\partial \boldsymbol{x}_i}\right) \frac{\partial S(X)}{\partial \boldsymbol{x}_i} + \sum_j \frac{\partial}{\partial \boldsymbol{x}_j} \sum_i \frac{\boldsymbol{p}_i}{m_i} \frac{\partial S(X)}{\partial \boldsymbol{x}_i} = 0 \tag{S7}$$

replacing S9 into S11,

$$\sum_i \boldsymbol{F}_i \frac{\partial S(X)}{\partial \boldsymbol{x}_i} = \lambda \sum_i \frac{\partial S(X)}{\partial \boldsymbol{x}_i} \frac{\partial S(X)}{\partial \boldsymbol{x}_i} \tag{S8}$$

and finally arrived at the desired expression

$$\lambda = \frac{\partial U}{\partial S} = \frac{\sum_i \boldsymbol{F}_i \frac{\partial S}{\partial \boldsymbol{x}_i}}{\sum_i \frac{\partial S}{\partial \boldsymbol{x}_i}\frac{\partial S}{\partial \boldsymbol{x}_i}} \tag{S9}$$

Charge transfer and the zwitterion

This section employs the Hirshfeld[3] partitioning to estimate atomic charges and show that the (metastable) species formed during CO_2 chemisorption in liquid ammonia is indeed a zwitterion. As shown in Fig. S2, the -CO_2 and the -NH_3 group of the molecule have same charge magnitudes but opposite sign. This observation corroborates the charge transfer between NH_3 and CO_2 during the formation of the zwitterion intermediate. For completeness, we have also performed the charge analysis on all chemical states involved during CO_2 chemisorption in liquid ammonia.

The charge analysis was performed on a set of approximately 40 configurations per chemical state extracted from the local minima in Fig.2 of the main text. The atomic charge on each atom shown in Fig. S2 is computed as the average charge over the selected configurations. For each of these configurations, a SCAN SCF calculation was performed using the same parameters listed in the methods section and the Hirshfeld charges computed. We note that the atomic charge is not a well-defined concept, since it depends on a non-unique methods to partition volume and assign electronic charge to specific atoms. The analysis performed here should therefore be taken as a qualitative measure of charge transfer resulting from the formation of the zwitterion intermediate. We also note that the sum of the atomic charges of the physisorbed CO_2 molecule does not add to zero, indicating either some degree of charge transfer from CO_2 to the nearby solvent environment or an artifact of the Hirshfeld volume partitioning.

Free CO_2

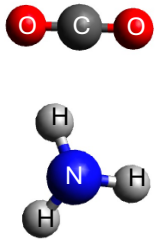

C	0.92(3)
N	-1.12(1)
O	-0.39(3)
H	0.37(1)

Zwitterion

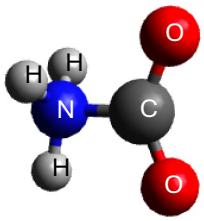

C	1.02(1)
N	-1.08(4)
O	-0.61(2)
H	0.42(2)

Carbamate

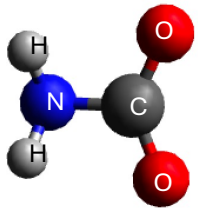

C	1.04(1)
N	-1.08(3)
O	-0.64(2)
H	0.40(1)

Carbamic acid

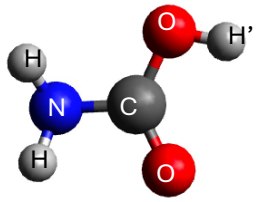

C	1.05(1)
N	-1.06(3)
O	-0.62(3)
H	0.42(1)
H'	0.44(1)

Figure S2: Average Hirshfeld atomic charges of the 4 chemical states (labels A-D in Fig. 2 of the main text) extracted from the enhanced sampling simulations of CO_2 chemisorption in liquid ammonia. Numbers in parenthesis indicate the standard deviation in the last reported digit (obtained from the deviation over the atomic charges computed from approximately 40 configurations). Values of charge are shown in elemental charge units.

Generalization of the free energy sampling to substituted amines

The free energy sampling method applied to study the CO_2 chemisorption in liquid ammonia can be straightforwardly generalized to other amines. This section employs the same methodology described in the main text to sample the CO_2 chemisorption in two substituted amines: methylamine and dimethylamine. The only purpose of the results shown in Fig. S3 is to prove the generalizability of the methodology proposed in the main text, since no validation of the machine learning potential is made here for methylamine and dimethylamine. As seen in Fig. S3, the same method used to sample the CO_2 chemisorption in liquid ammonia can also be applied to study this reaction for substituted amines.

The sampling of CO_2 chemisorption in methylamine and dimethylamine required the extension of the original training data described in the main text. The same active learning

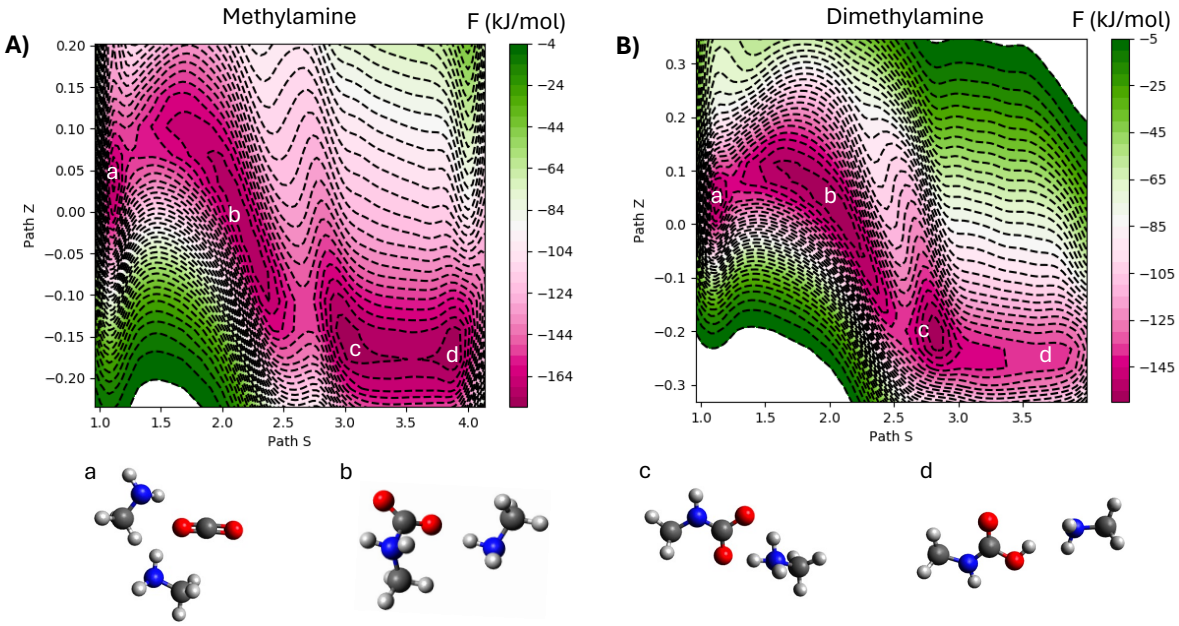

Figure S3: Free energy surface of CO_2 chemisorption in (A) methylamine and (B) dimethylamine. Cartoons in the bottom panel display the chemical states a-d (using methylamine only) shown in panels A and B. Results were obtained at 300 K and constant volume. The path collective variables S and Z are described in detail in the methods section of the main text.

approach used to train liquid ammonia was also applied to sample configurations for methylamine and dimethylamine. A more systematic study on the effect of substitution on the affinity of CO_2 for amines will be presented in a forthcoming publication.

References

(1) Sadus, R. J. *Molecular simulation of fluids*, 2nd ed.; Elsevier, 2023.

(2) Frenkel, D.; Smit, B. *Understanding Molecular Simulation*, 2nd ed.; Academic Press San Diego, 2002.

(3) Bultinck, P.; Alsenoy, C. V.; Ayers, P. W.; Carbó-Dorca, R. Critical analysis and extension of the Hirshfeld atoms in molecules. *Journal of Chemical Physics* **2007**, *126*.